

Hubble Space Telescope Fine Guidance Sensor Post-Flight Bearing Inspection

J. Pellicciotti*, S. Loewenthal**, W. Jones Jr.+ and M. Jumper**

Abstract

Aerospace mechanism engineering success stories often, if not always, consist of overcoming developmental, test and flight anomalies. Many times it is these anomalies that stimulate technology growth and more reliable future systems. However, one must learn from these to achieve an ultimately successful mission.

It is not often that a spacecraft engineer is able to inspect hardware that has flown in orbit for several years. However, in February 1997, the Fine Guidance Sensor-1 (FGS-1) was removed from the Hubble Space Telescope (HST) and returned to NASA Goddard Space Flight Center (GSFC) during the second Servicing Mission (SM2). At the time of removal, FGS-1 had nearly 7 years of service and the bearings in the Star Selector Servos (SSS) had accumulated approximately 25 million Coarse Track (CT) cycles. The main reason for its replacement was due to a bearing torque anomaly leading to stalling of the B Star Selector Servo (SSS-B) when reversing direction during a vehicle offset maneuver, referred to herein as a Reversal Bump (RB). The returned HST FGS SSS bearings were disassembled for post-service condition assessment to better understand the actual cause of the torque spikes, identify potential process/design improvements, and provide information for remedial on-orbit operation modifications.

The methods and technology utilized for this inspection are not unique to this system and can be adapted to most investigations at varying stages of the mechanism life from development, through testing, to post flight evaluation. The systematic methods used for the HST Fine Guidance Sensor (FGS) SSS and specific findings are the subjects presented in this paper. The lessons learned include the importance of cleanliness and handling for precision instrument bearings and the potential effects from contamination. The paper describes in detail, the analytical techniques used for the SSS and their importance in this investigation. Inspection analytical data and photographs are included throughout the paper.

Introduction & FGS Description

Hubble's three FGS's — its targeting cameras — provide feedback used to maneuver the telescope and perform celestial measurements. Two of the sensors point the telescope at an astronomical target and then hold that target in a scientific instrument's field of view. The third sensor is available to perform scientific observations. The sensors aim the telescope by locking onto "guide stars" and measure the position of the telescope relative to the object being viewed. Adjustments based on these constant, minute measurements keep Hubble pointed precisely in the right direction.

Each FGS enclosure houses a very precise optical interferometer. The pointing control system uses the Fine Guidance Sensors to point the telescope at a target with an accuracy of 0.01 arcsec. The sensors detect when the telescope drifts which gives Hubble the ability to remain pointed at that target with no more than 0.007 arcsec of deviation over long periods of time. This level of stability and precision is like being able to hold a laser beam focused on a dime 320 km (200 miles) away (about the distance from Washington, D.C. to New York) for 24 hours.

The Star Selector Servos "A" and "B" assemblies move independently of each other to affect the tilt of the wave front through the instrument. Each SSS is comprised of a brushless DC motor and 21-bit encoder

* NASA Goddard Space Flight Center, Greenbelt, MD

** Lockheed Martin Space Systems Company, Sunnyvale, CA

+ SEST Inc., Middleburg Heights, OH

** BEI Precision Systems & Space Division, Maumelle, AR

(M/E assembly), supported by a duplex pair set of thin section angular contact bearings (see Figures 1 & 4). The M/E duplex pair (DB) bearing is made up of an “A” bearing and “B” bearing. The inner, and outer spacers, races, and balls were manufactured with passivated, CEVM 440C Stainless Steel. The bearing conformity ratio is 52.5% (race radius / ball diameter). The races and 88 balls per bearing were treated with Tricresyl Phosphate (TCP) for 72 hours at 107°C (225°F) per federal specification (TT-T-656). Each bearing was lubricated with approximately 240 milligrams of Bray 815Z oil in November 1981 by Split Ballbearing. Both spacers were grease plated with Braycote 3L-38-RP, a teflon thickened grease using Brayco 815Z base oil. The bearing separators are Teflon toroids around alternate balls. Throughout this paper, references will be made to the two sets of bearings for each FGS Servo in the following manner:

| FGS Servo | Motor/Encoder | Bearing Assy. | Bearing Pair |
|-----------|---------------|---------------|--------------|
| A | 3009 | 007 | 0-107 A & B |
| B | 3010 | 008 | 0-106 A & B |

Previous engineering findings by Stu Loewenthal et al^[2] from ground-based life tests identified that a build-up of degraded lubricant from excessive CT cycling caused a “bump” for the ball to roll over prior to continuing to its required position (Figure 2). This bump caused a spike in the motor voltage as indicated by the Compensated Error (CE) signal, which is a direct indication of a high torque. This CT torque bump, occurring at nominal 9.8 degree ball defect spacing, has been observed to some extent on all FGS bearings, but primarily on A servos due to the method for sampling the CE signal. However, the principal reason for refurbishing FGS-1 was due to servo-B repeatedly stalling after direction reversal during vehicle offset slews (Figure 3). Unlike CT bumps, the exact cause of this “reversal” bump (RB) remained unknown although believed to be a distinctly different type of bearing anomaly, possibly related to internal or foreign debris. Only FGS -1B and -3B exhibited this problem, with FGS-3B in an early stage. However, FGS-3B is still in operation.

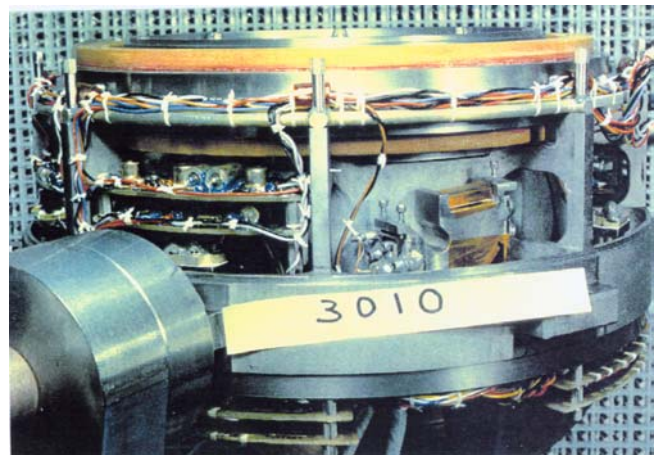
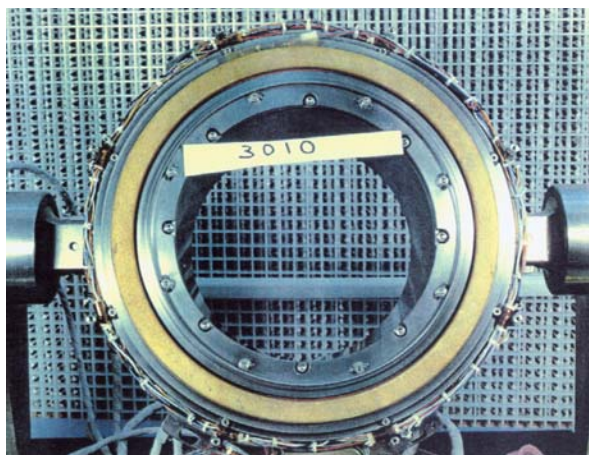


Figure 1. SSS Motor/Encoder assembly (Top). HST FGS-1 SSS-B after cover removal (Bottom) ^[3]

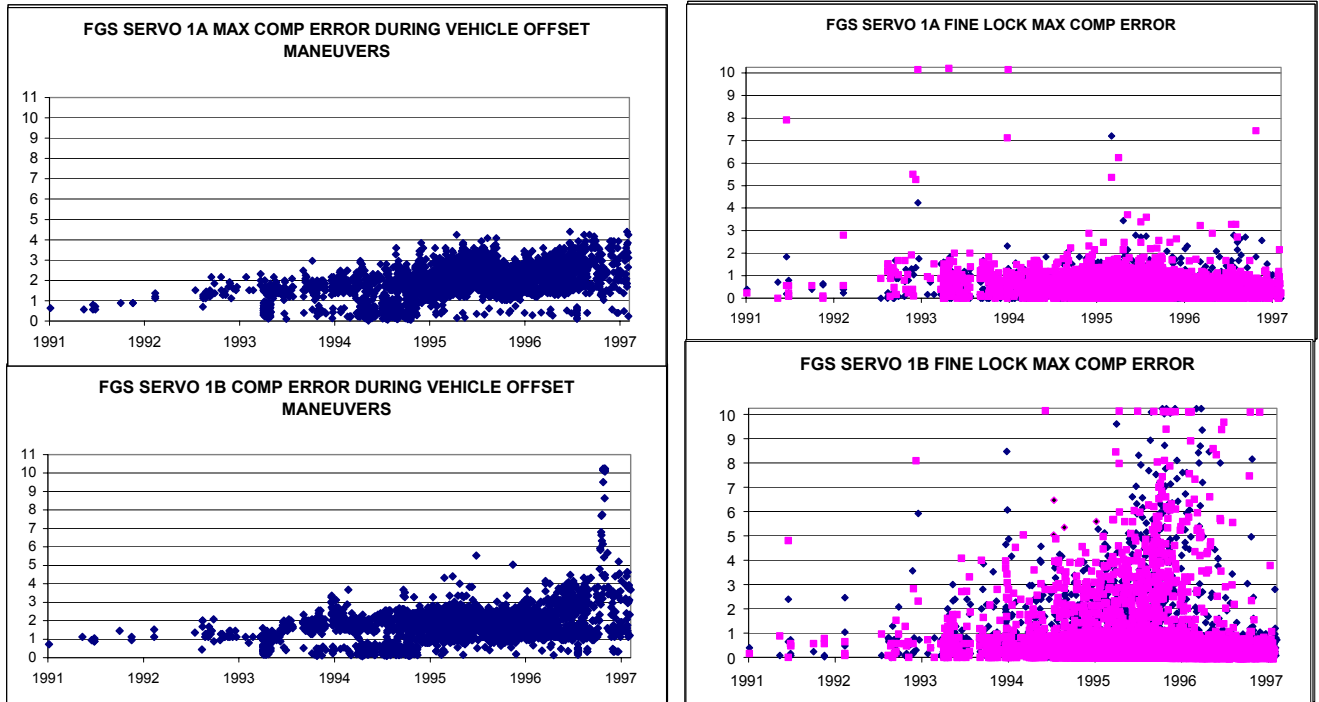


Figure 2. Max Compensated Error (CE) during vehicle offset maneuvers showing CT bumps (Left), and during Fine Lock showing Reversal Bumps (Right). Note: motor stall can occur above 10V Comp Error.

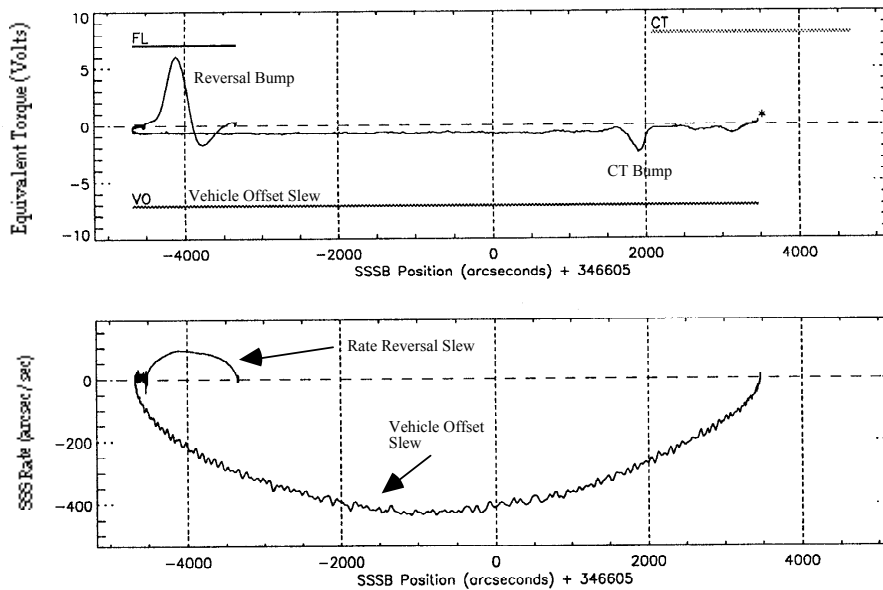


Figure 3. Example of FGS-1 SSS-B Reversal Bump. Initial direction of motion is right to left. Note CT bump at end of CT stroke (bar, upper panel). Direction reverses at a position of about -4,700 arcseconds and a 6.1-volt Reversal Bump forms. [2]



Figure 4. FGS-1 Motor/Encoder SSS-A bearing assy. Encoder optical disk shown (white particulate identified by white arrows) (Left). Clamp Ring removed and 0107B bearing exposed for inspection (Right).^[1]

Inspection Planning & Technology

The objective of the disassembly and inspection of the SSS assemblies were to verify the cause of the CT bump anomaly, but even more importantly, determine the cause of the reversal bump anomaly since it was felt that ground testing well characterized the CT anomaly but could never accurately explain the cause of the reversal bumps. After return of the FGS instrument from SM2 to the HST test facility at GSFC, several ground tests were performed at the instrument assembly level in an attempt to reproduce the on-orbit anomalies. The CT bumps encountered were similar to that on-orbit, although much smaller in magnitude. Reversal Bumps were much smaller than those observed on-orbit (4.4V maximum vs. 10V saturation). By the third day of testing, the Reversal Bumps disappeared and the CT bumps were less than 2V peak.

At the completion of instrument level testing, the M/E's were removed and sent to their manufacturer for additional testing and tear down to the bearing assembly level. Once the motors and encoder electronics were removed, the units were sent to the Material Analysis Laboratory at Lockheed Martin for detailed inspection. The inspection/operations flow is outlined in Figure 5.

The process of planning and creating the procedure for the inspection was critical to having a comprehensive flow that provided the best chance for resolving the anomaly causes. A good plan results in the most efficient use of time during the inspection and test process when support personnel are at the peak and critical equipment must be scheduled around other tasks.

The first step was to determine the most probable causes of the anomalies from the available data. This provides a focus on the task, but should not limit the ability to shift focus onto other areas of concern or potential causes. Conclusions should not be drawn here, but allow for a wide range of *probable* and *likely* reasons for the anomaly. All relevant drawings, test and flight data should be collected and reviewed in support of these hypotheses.

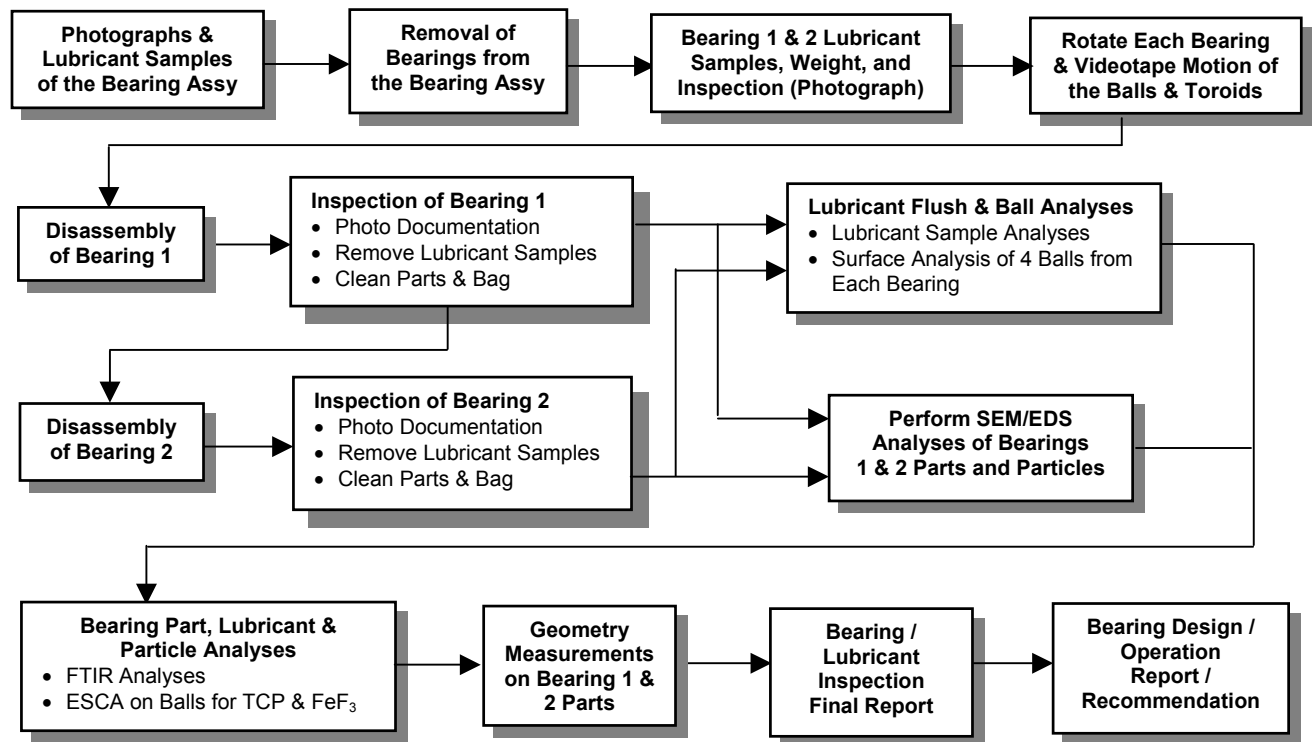


Figure 5. Bearing Inspection and Operation Flow

It is a rare occasion that the nominal acceptance or qualification tests will be sufficient for investigating a specific mechanism anomaly. Therefore, a test plan should be generated to gather more detail regarding the likely causes of the anomaly. Once the unit is torn down, it is probable that it could never be reassembled in a way that would reproduce the identical anomaly. Generally, mechanism torque information can be deduced from motor current amplitude and profile, motor voltage levels, torque transducer tests, and velocity tests. Position accuracy tests can provide an indication of mechanism wear, slop or hardware failure. Often, these tests may need to be run at operational environmental temperature and vacuum conditions to obtain accurate data. Other testing may be necessary based on the specific functions of a mechanism. The key is to be familiar enough with the mechanism and the analytical techniques available to completely evaluate the unit.

Once the test program is complete and the unit disassembly has begun, there are several methods available for investigation of the moving mechanical parts such as the bearings and lubricant in the case of the FGS SSS. It is important to take contamination and lubricant samples at various points throughout the tear down process since these may later provide an indication of anomaly sources. Samples can be taken by using a clean swab on the surface, performing a Freon or IPA (Isopropyl Alcohol) filtered rinse or simply removing a large particle using a clean tool such as dental pick or tweezers. Techniques for hardware surface and contaminant analysis used for the FGS Servos include FTIR, SEM/EDS, XPS (or ESCA), ICP/MS and OLM (defined below). Component weights should always be included in the process when lubricant quantities are in question. However, caution should be used in drawing conclusions from mass measurements since lubricant amounts can be extremely small and lubricant loss can be replaced by contaminants resulting in a false inference.

FTIR (Fourier Transform Infrared) Spectroscopy Analysis provides detailed molecular information on organic complexes and some inorganic groups, thereby aiding in material identification. The instrument

used was capable of examining areas as small as 10 μm , making it feasible to examine microscopic particles, fibers and small quantities of residues. FTIR is also useful for identifying lubricant degradation products.

SEM (Scanning Electron Microscope) equipped with an EDS (Energy Dispersive Spectroscopy) system is used to identify elemental composition of particles such as metallic debris found in bearings. It is also used to evaluate bearing race, ball and separator damage and potential causes at high magnification levels.

ESCA (Electron Spectroscopy for Chemical Analysis) provides compositional information from the top 5 nm of the surface region. Precise measurement of photoelectron binding energies provides the chemical state of surface atoms. Compositional information below the uppermost surface layers was obtained by ESCA in conjunction with argon ion sputtering.

ICP/MS (Inductively Coupled Plasma/Mass Spectrometry) typically detects 65 different elements at parts-per-million (ppm) levels. For the FGS M/E investigation, samples of the white residues from the clamp rings, submitted in plastic snap-cap tubes, were dissolved in 3 mL of 1% ultra-pure nitric acid. Control tubes were treated in the same manner along with the sample residues to check for background contamination. The nitric acid solutions were analyzed using the semi-quantitative feature of a Hewlett Packard Model 4500 ICP/MS (LIMS procedure ICPMS_SEMIQUANT). This method of analysis is generally accepted to be accurate to within ± 20 to 30% of the actual analyte values. The values obtained from this analysis were calculated to reflect the micro-grams of analyte per gram of sample as received ($\mu\text{g/g}$, or ppm).

OLM (Optical Light Microscopy) determines particle size distributions. These were done for the FGS Servos by manual inspection of filter samples of the debris collected from bearing flushes using a microscope equipped with a calibrated eyepiece reticule.

A determination of the logistical requirements for the anomaly investigation should be completed prior to commitment for execution of the plan. This includes facility requirements (floor space, cleanliness, handling of hazardous material (safety requirements)), wipes, swabs, required chemicals for cleaning or flushing debris, debris filters, glassware, packing materials, etc. Disassembly tools and Ground Support Equipment (GSE) necessary for the pre and post inspection tests, and tear down must be considered. In scheduling the task, individual support personnel should be identified by name and their availability confirmed. Finally, a realistic schedule should be generated that lists the major tasks to be performed with allowance for minor deviations resulting from in-process findings.

A final report deadline should also be identified and closely tracked. Since often the cause of an anomaly is not obvious, it is important to scour through all of the inspection data while it is fresh and there is an opportunity for more to be done. Creation of the final report provides a vehicle for systematically analyzing the data collectively to draw valid conclusions and report them to the interested parties.

Below is a general summary outline for the steps necessary in planning a mechanism anomaly investigation. Although some of the items discussed here were specific to the HST FGS M/E anomaly investigation, it can be used as a guideline in many other instances.

Inspection Planning Summary:

1. Determine the most probable cause for the anomaly.
 - a) Collect and review all relevant design drawings.
 - b) Collect and review all relevant test and flight data (if available).
2. Determine the desired testing program prior to tear down of the unit.
 - a) Thermal and/or vacuum environment required?
 - b) Motor current, voltage, torque transducer, velocity, position accuracy, operational vibration (accelerometer).
3. Surface, lubricant, and particle analysis techniques required to fully evaluate the unit to be inspected.

- a) These should include those required to verify the most probable findings in addition to other possible anomalies.
- b) Analytical Equipment includes: FTIR, SEM/EDS, ESCA or XPS, ICP/MS, OLM, and Gram Scales.
- c) Techniques to be used for taking samples.
 - 1) Surface swab samples.
 - 2) Manual extraction.
 - 3) Freon rinse and filter.
- 4. Determine the logistical requirements for the inspection.
 - a) Facility requirements (cleanliness, hazardous material, safety, etc.).
 - 1) Lab Coats, gloves, wipes, swabs, chemicals, debris filters, glassware, packing.
 - b) Tools and GSE needed for disassembly.
 - c) Available Personnel.
 - d) Schedule (provide sufficient time for changes to the plan based on findings).
- 5. Final Report

The outline above was not available for the HST FGS mechanism inspection; however, most of the steps listed were included in the initial planning process. The remaining detail, such as the actual analytical equipment used, was added during the inspection and documented in the final report.

FGS M/E Inspection & Findings

Prior to creating the FGS-1 M/E Inspection Plan, a general idea for the cause of the CT and RB anomalies was developed. It is difficult to predict what would be found during the detailed inspection and material analyses. However, industry tests in addition to the previously mentioned Life Tests^[2] provided a clue to what was expected. Therefore, the focus of this task became a lubricant and bearing degradation problem. It was anticipated that degraded lubricant would be found, however, the pertinent question was the cause of the degradation. Was it from a loading situation, contamination, operational scenario, workmanship, or some other phenomena?

Before the unit was disassembled, a battery of tests were conducted at the instrument level and the mechanism bench level^[3]. Table 1 provides a comparison between the performance of the M/E from its build Acceptance Tests in 1983 to its performance after removal from flight FGS-1 at the mechanism vendor's facility in 1998. It was concluded from this test data that there was a very slight degradation of positional accuracy in the motor encoders (probably due to degradation of the light output in the readstation LED's) but no other significant changes in performance was noted.

After all bench tests were completed, the M/E manufacturer disassembled the mechanism down to the bearing cartridge, which includes the housing, shaft, bearings and spacers. These are self-contained units, and it was not possible for contamination to enter this portion of the mechanism. The M/E's were then bagged, packed and shipped to the facility for final disassembly, detailed inspection and analyses.

After disassembly and inspection of the two M/E assemblies, the bearings were removed, visually inspected, photo-documented, and weighed. Some of the debris observed during the low magnification observations were lifted via probing and analyzed using a battery of analytical techniques, including FTIR, SEM, EDS, and ESCA (or XPS). Bearing motion testing was conducted to observe the behavior of the toroid ball separators under operation similar to on-orbit cycling. Subsequently the bearings were flushed to collect the remaining loose debris. Finally the bearings were disassembled, and the condition of bearing races, balls and toroids were evaluated visually under an optical microscope and with a SEM.

Both SSS-A and SSS-B bearings contained degraded lubricant residue, little to no free oil and were heavily contaminated with foreign fibers, metallic and non-metallic particles. None of the bearing components appeared to have experienced significant wear. With the exceptions that the lubricant in 0106 (SSS-B) bearings was slightly less degraded than the 0107 (SSS-A) bearings, and the 0107 bearings had less non-metallic particles (mostly skin), there was no other obvious differences between the relative condition of the bearings. The observed differences were insufficient to explain conclusively why the 0106 bearings in FGS-1B experienced reversal bumps and the A-servo did not. However, the

difference in location of the degraded lubricant on the toroid (faces of 0106 and bore / OD of 0107) with its observed motion during reversal provides a hypothesis of increased friction between the toroid and race land. The more degraded lubricant condition in the 0107 bearings is consistent with the observation that all of the A-side servos generally have more serious CT bump problems than the B-side servos. Figure 6 is photographs of the 0107 and 0106 bearings and lubricant degradation products.

Table 1. Star Selector Servo Subsystem Performance Test Data Comparison ^[3]

| TEST PARAMETER | FINAL PERFORMANCE TEST 9 NOVEMBER 1983 | | INCOMING EVALUATION 6 MARCH 1988 | |
|---|---|----------------------|-------------------------------------|----------------------|
| | ME 3009 & RU 4009 | ME 3010 & RU 4010 | ME 3009 & RU 4009 | ME 3010 & RU 4010 |
| Case Gnd to Circuit Gnd Isolation | > 10 Megohms | > 10 Megohms | > 10 Megohms | > 10 Megohms |
| Case Gnd to Case Gnd Pin Continuity | < 1 ohm | < 1 ohm | < 1 ohm | < 1 ohm |
| Running Torque (Comp. Error Signal): | | | | |
| Amplitude | Unknown (1) | Unknown (1) | 0.7 to 1.0 volts | 0.8 to 1.2 volts |
| Spikes in Trace | None | None | None | None |
| Direction of Rotation | | | | |
| Increasing Count | CCW | CCW | CCW | CCW |
| Decreasing Count | CW | CW | CW | CW |
| Sequence Test (SIGN Up) | No Errors | No Errors | No Errors | No Errors |
| Servo Bandwidth (Open & Closed Loop) | Acceptable | Acceptable | Acceptable | Acceptable |
| Power Dissipation | | | | |
| M/E (Motor On) | 5.07 watts | 5.03 watts | 5.16 watts | 5.06 watts |
| R/U (Motor On) | 4.04 watts | 3.54 watts | 3.59 watts | 3.51 watts |
| Total System Power (Motor On) | 25.79 watts | | 25.63 watts | |
| M/E (Motor Off) | 3.59 watts | 3.60 watts | 3.60 watts | 3.54 watts |
| R/U (Motor Off) | 4.08 watts | 3.63 watts | 3.55 watts | 3.48 watts |
| Total System Power (Motor Off) | 22.34 watts | | 21.94 watts | |
| Position Accuracy (Max. Peak-to-Peak Error) | 1.27 arc sec | 2.10 arc sec | 2.095 arc sec | 3.034 arc sec |

(1) 1983 Torque Traces were run without gridlines, so it is difficult to measure the exact amplitudes of the compensated error signal responses. Amplitudes are estimated to be between 0.5 and 1.0 volts for both motor encoders.

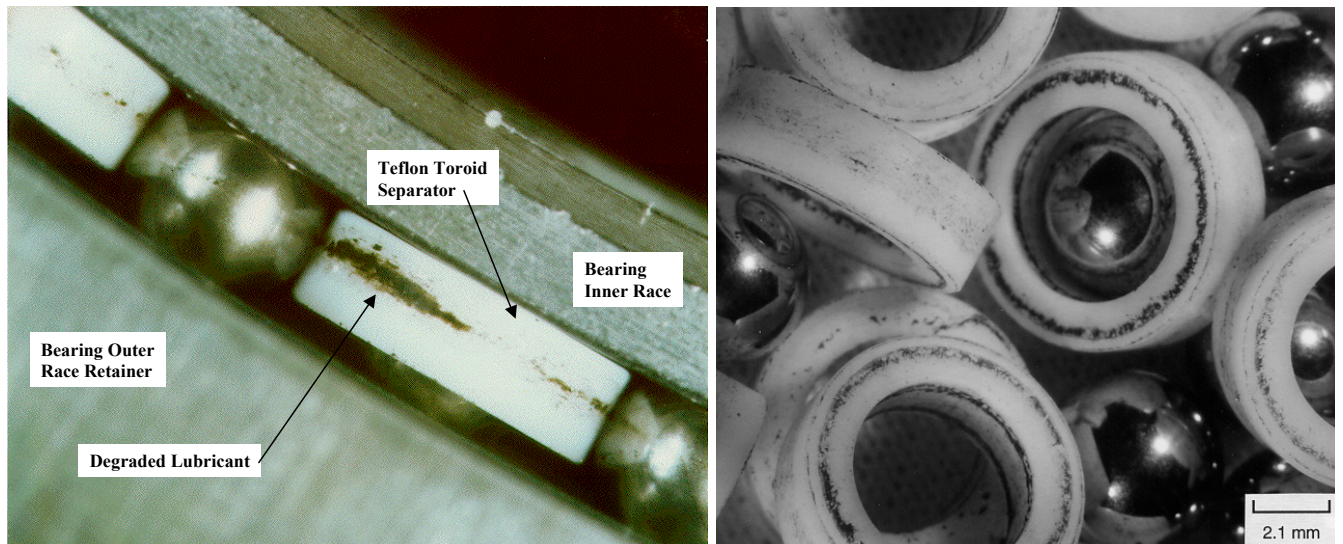
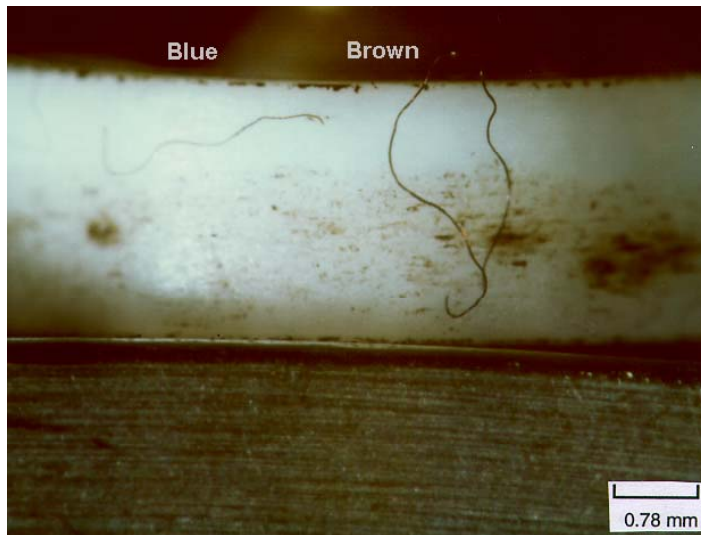


Figure 6. Bearing 0107B (SSS-A) mounted in bearing assembly housing (Left). Bearing 0106A (SSS-B), balls and toroids after bearing disassembly (Right). Note locations of degraded lubricant on the separator. ^[1]

There is no conclusive evidence that the foreign debris found in the FGS-1 bearings contributed to the problems observed on-orbit. It is surprising that torque spikes were not more prevalent during on-orbit service and during post-flight testing, considering the abundance of metallic and fibrous debris in both sets of bearings. It is unlikely that this debris was introduced during the inspection process, because strict attention was paid to contamination control during inspection. Also noteworthy are the observation of variety of contaminants with many types not even present in the inspection area, and less debris observed in the entry zone areas (such as the housing, clamp rings, etc.) as compared to that within the bearings. The presence of flattened fibers and metallic particles, and the extensive denting on the balls and races (potentially some of these inflicted by the debris) also indicate these are not artifacts introduced during disassembly. Although some of the aluminum particles could conceivably have been introduced from the aluminum motion tester, the flattened, plate-like appearance of the particles suggests that considerable torque would have been required. Furthermore, the energy required to roll over this debris would undoubtedly have caused hang-up of the motor. This suggests that the bulk of this damage likely occurred during early bearing run-ins prior to final instrument assembly. The following paragraphs describe the data achieved from each of the analytical techniques described in this paper.

Figure 7 shows the fibers from the 0106B bearing. Table 2 lists the fiber size distributions from each of the four bearings. Most obvious from the table is that the 0106B bearing flush has a greater number of fibers in each size-range class. Also, there were more fibers observed in the "B" bearings than in the "A" bearings. The entire filter surface was scanned at 50x magnification. As shown, a large number of fibers (>60 on each filter) were counted in the bearing-flush debris. To characterize, 8 to 9 fibers of different types were selected for infrared analysis. The infrared spectra show that the fibers from each of the bearings are predominately polyester and cellulosic based compounds. Several polyamide-based fibers (nylon 6 or 66 in some cases) and an acrylic fiber were also observed. Figure 8 shows the associated FTIR analysis for a particular fiber from this bearing.



M/E 3010, Bearing 0106B, Blue (left) and brown (right) fibers found on toroid prior to flushing. FTIR indicated blue to be cellulosic, and brown to be polyamide.

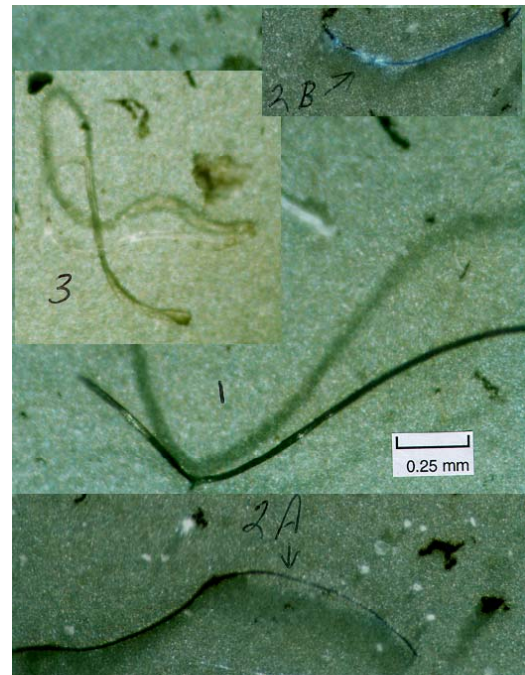
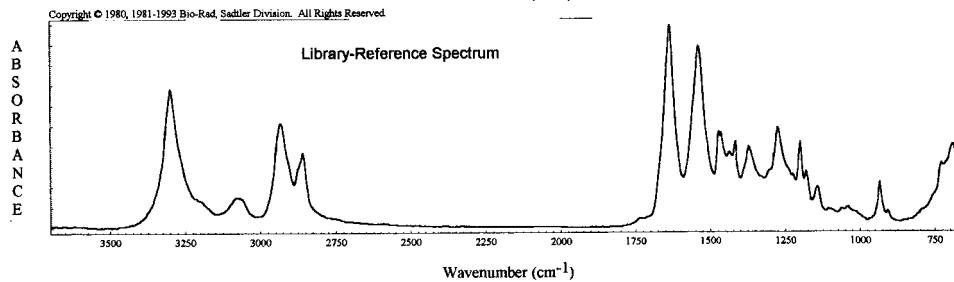
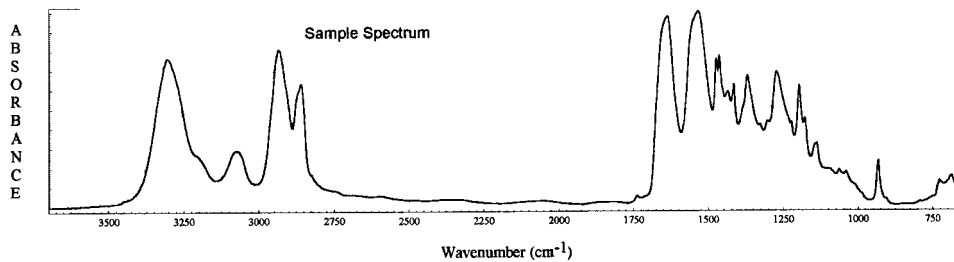


Figure 7. Bearing 0106B fibers removed from filter paper debris and analyzed by FTIR. [1]

Table 2. Fiber Size Distribution ^[1]

| Size Range, microns | 0106A Counts | 0106B Counts | 0107A Counts | 0107B Counts |
|---------------------|--------------|--------------|--------------|--------------|
| 100-250 | 12 | 20 | 8 | 18 |
| 251-500 | 22 | 53 | 24 | 37 |
| 501-1000 | 23 | 47 | 20 | 34 |
| >1000 | 10 | 28 | 13 | 11 |
| Totals | 67 | 148 | 65 | 100 |

AF1551S2.SPA



W1951 VYDYNE 66B HIGH MOLECULAR WEIGHT EXTRUSION GRADE NYLON 66

Figure 8. FTIR spectra of nylon library ref. (bottom) and fiber found in 0106B bearing (top). ^[1]

The bearing races, balls, and toroids were examined prior to additional cleaning using an Optical Light Microscope (OLM). The inner races and balls were also examined using Scanning Electron Microscopy (SEM). In both cases, too much residual lubricant was observed, that masked the wear or damage evaluation. Hence, the inner races and balls were further cleaned using Freon and a polyester swab and/or wiper to remove the residual lubricant. Due to the size limitation of the SEM chamber, only the inner races could be introduced into the SEM and examined; outer races were not examined.

Four balls per bearing were examined using SEM. The damage on the balls was similar to those observed on the races, except smaller, typically less than 20 micrometers. Multi-fragment dents and pits/pullouts were noted in at least one of the four balls from each bearing. The most prevalent damage in the ball track of the inner races, as observed using SEM, was indents. The indents typically ranged in size from 20-100 micrometers in diameter, a few were less than 20 micrometers. Some bearing inner races had indent patterns that were repeated on the same race which suggested that debris was able to cling to a ball or toroid as it rolled on the race. The Fringe, defined as plastically deformed metal at the edge of a pit or indent that resulted from excavated or plowed material, may be capable of causing repeated bumping during service, hence, the damage was categorized as with or without fringe. Figure 9 illustrates two examples of a damage fringe. One that has been rolled over during service operation and one that has not.

Flushed particles that appeared metallic were also analyzed by SEM / EDS to determine their origin. Figure 10 is an example of a 300 series stainless steel particle with a smooth surface. These surface characteristics indicate that the particle was most likely in the bearing raceway at some point and rolled over by the balls during operation. The origin of this particle is probably from the mechanism fasteners.

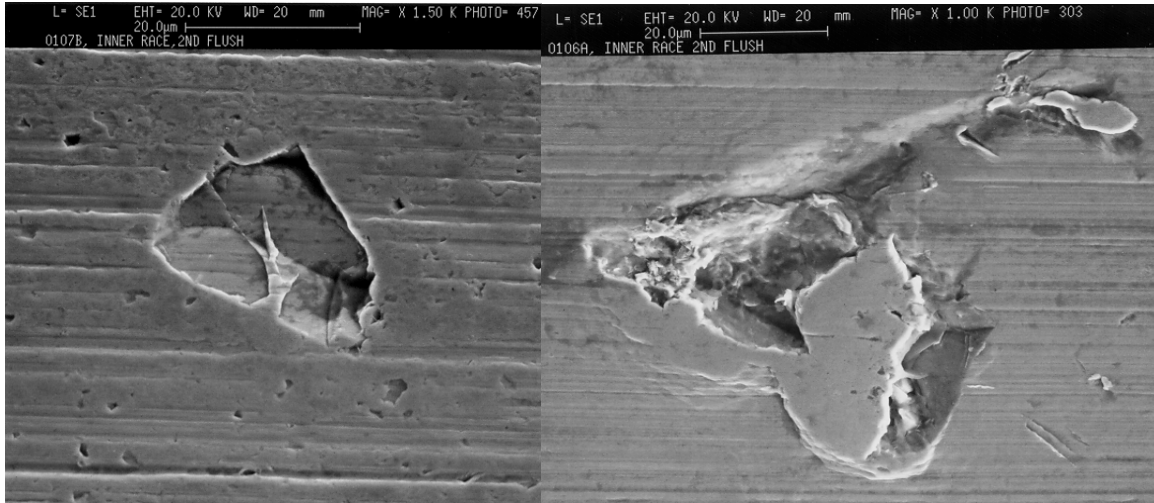
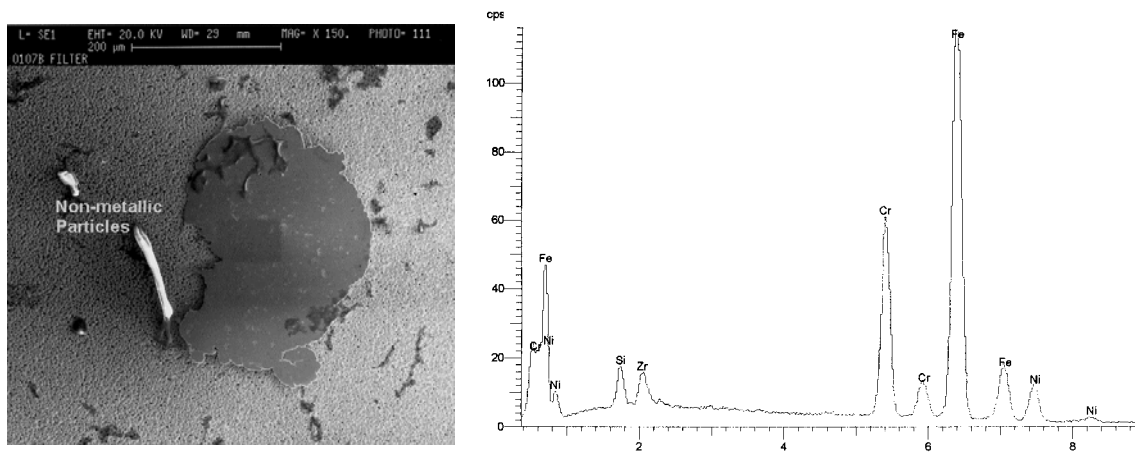


Figure 9. SEM photomicrograph of bearing 0107B indent without plastic deformation or without edge fringe (Left) and SEM photomicrograph of bearing 0106A with multi-fragment indent with plastic deformation or fringe (Right). [1]



Bearing 0107B, SEM micrograph (left) and corresponding EDS spectrum (right) of thick metallic particle, approximately 375 micrometers in length. EDS spectrum indicated Fe, Cr, Ni, and Zr, probably a 300-series stainless steel. Particle was thick enough to block filter paper Ag signal.

Figure 10. Bearing 0107B SEM of particle. [1]

ESCA (Electron Spectroscopy for Chemical Analysis) was used to examine the surface chemistry, and in particular to understand the presence of phosphorus reaction compounds (originating from TCP) and fluorine reaction compounds (from lube), if any. One ball per bearing was examined using ESCA. Table 3 summarizes the composition of the various ball surfaces after the initial Freon flush and after further flushing. The detection of ionic fluorine on the ball surfaces suggests lubricant breakdown and subsequent reaction with the metal(s) in the steel ball. The persistence of fluorine after flushes and

sonication suggests a potential strong bond of the lubricant with the steel. No phosphorous was seen on any of the ball surfaces, suggesting that it was either removed by surface wear during the bearing operation or the TCP treatment was inadequate. Race surfaces could not be examined for phosphorous due to limitation of physical size of the ESCA chamber.

Table 3. ESCA Results of Freon Flushed Bearing Balls ^[1]

| <u>Specimen</u> | <u>Composition (Atom %)</u> | | | | | | |
|----------------------------|-----------------------------|----------|----------|-----------|-----------|----------|-----------------------------------|
| | <u>F</u> | <u>O</u> | <u>C</u> | <u>Fe</u> | <u>Cr</u> | <u>N</u> | <u>Other</u> |
| #0106A, First flush | 44 | 21 | 30 | 3.7 | 0.5 | 0.4 | |
| #0106A, Second flush | 21 | 27 | 42 | 6.9 | 1.6 | 1.0 | |
| #0106B, First flush | 44 | 20 | 32 | 3.0 | 0.5 | 0.4 | |
| #0106B, Second flush | 21 | 24 | 48 | 4.6 | 1.7 | 0.9 | |
| #0107A, First flush | 46 | 20 | 30 | 3.0 | 0.6 | 0.3 | |
| #0107A, Second flush | 17 | 30 | 42 | 6.8 | 3.2 | 1.0 | |
| #0107B, First flush | 48 | 20 | 28 | 3.3 | 0.6 | 0.3 | |
| #0107B, Second flush | 23 | 24 | 45 | 5.4 | 2.5 | 0.9 | 0.1 Cu, 0.1 Cl |
| #0107B, Sonicated in Freon | 21 | 28 | 40 | 7.1 | 3.2 | 0.7 | 0.2 Cu, 0.3 Cl, 0.2 Na, 0.1 Mo |
| Braycote 815-Z | 57 | 18 | 25 | | | | |

A white-grainy material was observed on the shafts and clamp rings of both motor/encoders. The bearing clamp ring is machined beryllium S-200E, with no coating. The shaft material is also machined beryllium, but with an electroless Ni coating. After removing a small portion of the residue, the clamp rings were found to contain many small pits. Samples of the white residue were probed off both clamp rings, dissolved in 1% ultra pure nitric acid, and analyzed by ICP/MS (Inductively Coupled Plasma/Mass Spectrometry). High levels of beryllium were detected, however, due to the difficulty of isolating the white residues, only minute samples were tested thereby limiting the quantitative accuracy of the reported results.

During the investigation process, a report was found on a spare bearing set from the same lot as the flight units manufactured in the 1981 time frame. In 1987, this spare set was sent back to the manufacturer for refurbishment (well after assembly of the flight units). This refurbishment revealed contamination and debris particles in the bearing, rolled flat, of the same type found in the FGS-1 M/E's. The bearing races also showed evidence of brinelling. These spare bearings were subsequently cleaned, honed, and reassembled with new balls. The refurbished spare bearings functioned within specification requirements. It is thought that the metal partials described above were rolled flat probably during run-in at the bearing vendor prior to shipment. The contamination source may have been the solvents (unfiltered) used to clean the bearings prior to lubrication. It is surprising that all torque traces recorded during assembly of the flight mechanisms were in family and within requirements and that pre-disassembly torque traces showed essentially no evidence of the extensive debris in these bearings. Apparently, the debris was pushed out of the ball running track and content to stay in areas that didn't have much of an effect on torque.

Conclusions

The completed inspection as described herein resulted in several general findings for the FGS M/E bearings and some specific to each bearing. In general, no evidence of the anti-wear additive (TCP) was found on the bearing balls. The bearings appeared dry (some more than others) with degraded, "black tar

- like," lubricant with the degraded lubricant adhered to the races and toroids. There was a slight oil film noted around the balls when viewed under microscope at ~6x. Hundreds of skin particles and fibers were found in bearing flush filters. Many metallic particles were also found on the bearing flush filter and analyzed by SEM/EDS. Most particles were determined to be 300 - series stainless steel, galvanized steel, carbon steel, 6000 - series aluminum and brass. SEM results on the bearing races revealed damage (recorded only if in wear track) characteristics of indentations with fringes, indentations without fringes, multi-fragment dents with fringes, multi-fragment dents without fringes, repeated dent patterns, pits / pullouts and multi-fragment dents on the balls, and detection of ionic fluorine on ball surface that suggests lubricant breakdown. It was also observed during the bearing rotation test that the toroids tend to wobble from inner to outer race when the bearing reverses direction and at least one toroid in bearing 0-106A appeared to skip across the race land as the bearing rotated.

There is no conclusive evidence that the foreign particles alone contributed to the on-orbit anomalies. There were no torque spikes during initial build and test. The post flight torque traces were mostly clean, although not unexpected, the torque noise on the traces was about 30% larger, probably due to lack of lubricant, contamination, and damage to balls and raceways over life. The FGS life test bearings showed CT bumps without contamination - only degraded lubricant. The presence of numerous flat fibers and metal particles in the bearing and smooth torque traces show that the bearing run-in and functional testing flattened the particles and permitted smooth performance. All FGS bearings yielded smooth torque traces initially even though they most likely contain particles. Degraded lubricant was most significant contributor to an on-orbit Coarse Track torque increase. Degradation debris collected at the end of each stroke caused a bump for the ball to roll over. This was evident from the CT anomaly reproduced in life tests at Lockheed Martin Space Systems Company (LMSSC) in 1994^[2]. Operational changes in 1994 significantly reduced CT cycles.

Reversal Bumps were never reproduced during life testing at LMSSC in 1994 and ground tests on FGS-1 at the GSFC VEST facility, post SM2, were never able to reproduce the magnitude of RB's seen on orbit. After three days of tests, the existing RB's disappeared. There was inconclusive evidence from inspection to explain reversal bump phenomena; however a hypothesis is that a combination of degraded oil, dry bearing, particulate debris and blocking caused the Reversal Bumps. Reversal bump characteristics occurred at ~0.128 degrees (460 arcsec.) after reversal, suggesting a very steep torque slope. This indicates that a foreign particle may be caught between the ball and race upon reversing direction. As the ball rotates in one direction, the toroid edge acts as a wiper pushing a particle along the surface of the ball. When direction is reversed, this particle stays with the ball and gets wedged between the ball and raceway creating the RB. Also, an error or misalignment in the ring can cause the ball to spin and the contact angle to fluctuate as it travels around the bearing. The change in contact angle causes varying ball speeds that result in the balls applying load to each other (*Blocking*^[4]), leading to increased torque. As a result of this inspection exercise, several recommendations were made for the rebuild of the future FGS M/E's. These included bearing race conformity changes to reduce the ball spin, reducing the likelihood of blocking and similar oscillatory torque anomalies. Verification of adequate application of anti-wear additive coatings where a control sample from the treatment may be required to validate the adequacy of the process. Strict contamination control requirements for processing and handling of the bearings and bearing assemblies. Finally, addition of more lubricant to the bearings.

The methods and technology utilized for this inspection are not unique to this system and can be adapted to most investigations at varying stages of the mechanism life from development, through testing, to post flight evaluation. The systematic methods used for the HST FGS SSS and specific findings are the important subjects of this paper. The lessons learned from the hardware include the importance of cleanliness and handling for precision instrument bearings and the potential effects from contamination. The analytical techniques used for the SSS inspection and their importance in this investigation should be considered as a template for future anomaly studies.

Acknowledgement

The authors would like to acknowledge the invaluable contributions for the support and state-of-the-art methods used by the Lockheed Martin Materials and Failure Analysis Team and in particular Dr. A. Joshi who organized the lab work.

References

1. Joshi, A., Christensen, P., Jurta, R., Loewenthal, S., & Pellicciotti, J., *HST FGS-1 Star Selector Servo Bearing Inspection*, LMSSC/P505033, 4 September 1998.
2. Loewenthal, S., Esper, J., Pan, J., & Decker, J., *Space Telescope Fine Guidance Sensor Bearing Anomaly*, 30th Aerospace Mechanisms Symposium, NASA CP 3328, pp13-29, May 1996.
3. BEI Sensors & Systems Co., *Preliminary Evaluation Report for the As-Received Condition of Motor/Encoders S/N's 3009 & 3010 and Remote Units S/N's 4009 & 4010 Returned from the Hubble Space Telescope's Fine Guidance Sensor / Radial Bay Module S/N 2002*, 2 July 1998.
4. Todd, M.J., European Space Tribology Laboratory, UKAEA, Risely, England, *Investigation of Torque Anomaly in Oscillating PDM Bearings*, ESA (ESTL) 49, May 1981.